Gradient-Based Fingerprinting for Indoor Localization and Tracking

Yuanchao Shu, *Member, IEEE*, Yinghua Huang, Jiaqi Zhang, Philippe Coué, Peng Cheng, *Member, IEEE*, Jiming Chen, *Senior Member, IEEE*, and Kang G. Shin, *Life Fellow, IEEE*

***Abstract*—Of the different branches of indoor localization research, WiFi fingerprinting has drawn significant attention over the past decade. These localization systems function by comparing WiFi received signal strength indicator (RSSI) and a pre-established location-specific fingerprint map. However, due to the time-variant wireless signal strength, the RSSI fingerprint map needs to be calibrated periodically, incurring high labor and time costs. In addition, biased RSSI measurements across devices along with transmission power control techniques of WiFi routers further undermine the fidelity of existing fingerprint-based localization systems. To remedy these problems, we propose Gradlent FingerprinTing (GIFT) which leverages a more stable RSSI gradient. GIFT first builds a gradient-based fingerprint map (Gmap) by comparing absolute RSSI values at nearby positions, and then runs an online extended particle filter (EPF) to localize the user/device. By incorporating Gmap, GIFT is more adaptive to the time-variant RSSI in indoor environments, thus effectively reducing the overhead of fingerprint map calibration. We implemented GIFT on Android smartphones and tablets, and conducted extensive experiments in a five-story campus building. GIFT is shown to achieve an 80 percentile accuracy of 5.6 m with dynamic WiFi signals.**

***Index Terms*—Fingerprinting, indoor localization, WiFi.**

I. Introduction

EMERGENCE of location-based services and applications has led to a growing demand of *anywhere* localization [2], [17], [28], [40], [48]. Although space-based satellite navigation systems such as GPS offer high localization accuracy outdoor, the poor connectivity between satellites and end-devices makes them unavailable indoor, triggering research on indoor localization.

Numerous approaches in indoor localization have been proposed using inertial measurement unit (IMU) [20], ultrasonic [6], [17], radio-frequency (RF) ID tags [28], [42], [43], FM [45], magnetic field [7], [19], WiFi [26], etc. Among different branches of techniques, fingerprinting approaches based on WiFi received signal strength indicator (RSSI) have attracted the most attention over the last decade. In such systems, an RSSI signature database (a.k.a. fingerprint map) needs to be constructed first in the training phase. User location is then obtained according to the results of comparing RSSI observations and the position-specific fingerprint map. WiFi fingerprinting systems are known to be accurate and free of additional infrastructures and specific hardware [45]. However, they suffer from several shortcomings, of which the WiFi signal variation is a major hurdle.

WiFi signal strength is subjected to indoor environmental changes. In addition to these probabilistic temporal variations, recent technologies implemented in off-the-shelf access points (APs) also cause difficulties in large-scale deployments of existing RSSI-based indoor localization systems. For example, in the AP-220 series APs, Aruba Networks implements adaptive radio management (ARM) which could monitor the ambient RF environment and automatically adjust transmit power to optimize the overall network performance [14]. Similar technologies could also be found in the equipments of other networking vendors such as Netgear [16] and Cisco [15]. Device diversity [11], [25] is another issue in WiFi-based fingerprinting systems where signal strength variations are observed among different devices. Due to unpredictable environmental changes, and limited *a priori* knowledge on both the sensing device and the power adjustment strategy, the RSSI fingerprint map needs to be periodically calibrated, incurring high costs on both labor and time.

Recent technological advances improved the efficiency of WiFi fingerprint map construction [26], [29], [30], [44]. For example, crowdsourcing is used to reduce the overhead of site profiling by distributing the workload among multiple mobile users [26], [44]. Floor maps and indoor landmarks have also been exploited for fast and unsupervised site profiling [29], [37]. Although these efforts improved fingerprint map construction, they still cannot deal with uneven fingerprint density and device heterogeneity, and therefore cannot adapt to the variations in AP transmission power, let alone reducing the frequency of the map construction to eliminate time-consuming and labor-intensive database maintenance.

Manuscript received January 10, 2015; revised April 25, 2015; accepted June 25, 2015. Date of publication December 17, 2015; date of current version March 8, 2016. This work was supported in part by the 973 Program of China under Grant 2015CB352503, and in part by the National Program for Special Support of Top Notch Young Professionals. *(Corresponding author: Jiming Chen.)*

Y. Shu was with the State Key Laboratory of Industrial Control Technology, Zhejiang University, Hangzhou 310027, China. He is now with Microsoft Research Asia, Beijing 100080, China (e-mail: yushu@microsoft.com).

Y. Huang, J. Zhang, P. Cheng, and J. Chen are with the State Key Laboratory of Industrial Control Technology, Zhejiang University, Hangzhou 310027, China (e-mail: huangyinghua@huawei.com; jiaqizhang@zju.edu.cn; pcheng@iipc.zju.edu.cn; jmchen@iipc.zju.edu.cn).

P. Coué is with Capgemini Telecom and Media, 75011 Paris, France (e-mail: king.pcoue@gmail.com).

K. G. Shin is with the Department of Electrical Engineering and Computer Science, University of Michigan, Ann Arbor, MI 48109 USA (e-mail: kgshin@umich.edu).

Color versions of one or more of the figures in this paper are available online at http://ieeexplore.ieee.org.

Digital Object Identifier 10.1109/TIE.2015.2509917

To deal with these problems, we propose a GradIent FingerprinTing (GIFT) indoor localization and tracking system. The basic rationale behind GIFT comes from the observation that differential RSSI between nearby positions is more stable than the absolute RSSI values, and more importantly, is independent of the AP's transmission power and the sensing device. For example, in an ideal RF environment, as the user is walking toward an AP, he will obtain increasing RSSI measurements with high probability, regardless of the AP's absolute transmission power and model of the sensing device.

Unlike several existing calibration approaches, no assumptions on the RSSI variation model caused by environmental changes and device diversity (e.g., linear relationship [13], [18]) are made in this paper. Instead, we extract the *binary RSSI gradients* from the RSSI fingerprint map, and establish the gradient fingerprint database (Gmap), leveraging statistical hypothesis testing methods. This way, GIFT is able to deal with both the time-varying effects and diverse RSSI measurements from heterogeneous devices, thus dramatically reducing the overhead of periodical maintenance of the fingerprint map. Besides Gmap, we design an extended particle filter (EPF)-based GIFT engine which simultaneously detects user movements and tracks the user's position.

The contributions of this paper are summarized as follows.

1) Based on the observation of the WiFi signal strength fluctuation, we proposed a novel indoor localization and tracking system using the RSSI gradient, i.e., GIFT. Unlike existing work which focuses on the design of either efficient fingerprint map building or calibration across heterogeneous clients, GIFT relies on simpler binary RSSI gradient values.
2) We develop a novel method to construct the binary Gmap on top of the WiFi RSSI fingerprint map using significance testing. It is backward compatible with existing, advanced fingerprint map construction approaches which could further reduce the training overhead.
3) We design an EPF-based GIFT engine with a motion detection module. It automatically locates and tracks the user and is adaptive to different mobility patterns.
4) We have implemented GIFT, as well as two legacy WiFi fingerprinting methods on smartphones and tablets, and conducted extensive experiments in a five-story campus building. The experimental results demonstrate high localization accuracy and robustness of GIFT in complex indoor WiFi environments.

This paper is organized as follows. Section II summarizes the related work first and Section III motivates GIFT with preliminary observations on WiFi RSSI in indoor environments. Section IV presents an overview of GIFT design. Sections V and VI detail the gradient-based map construction and the GIFT engine, respectively. Section VII presents the experimental evaluation of our proposed approach. Section VIII concludes this paper.

II. Related Work

Indoor localization has been extensively studied over the past decade. Here, we only focus on the systems related to GIFT.

WiFi-based fingerprinting has been discussed heavily in this area [1], [3], [34], [38], [46]. As a pioneering fingerprint-based indoor localization system, RADAR [1] first overhears and records broadcast packets from WiFi APs to build a location-specific fingerprint map. Localization can be achieved by performing lookups within a pre-established database. On the basis of basic fingerprinting, Horus [46] adopts a probability-based inference model, where the RSSI from an AP is modeled into a random variable in both time and spatial domains. Fingerprinting leveraging FM [3], [45] signals and magnetic field [7], [19] are also well studied. Despite the low cost on infrastructures, fingerprint-based approaches suffer from periodical onerous fingerprint map calibration caused by environmental changes. Although crowdsourcing techniques [26], [29], [44] could be used to reduce the cost, they do not take frequent and automatic configuration changes of WLAN APs into consideration. In GIFT, by replacing the absolute value-based fingerprint map with a gradient-based map, we minimize the overhead on repetitive site profiling without performance degradation.

Another issue of fingerprinting is the time-varying signal strength and biased observations reported by heterogeneous devices [31]. The authors of [11] proposed an automatic radio map generation mechanism for device-free localization. It requires full knowledge of the AP (e.g., the position, the transmission power, and the antenna radiation pattern) and the surrounding environment (e.g., RF propagation properties of common building materials) to handle transmission reflections and diffractions. In addition, the overhead of constructing the measured radio map is prohibitive when taking the human body effect into account in RF prorogation modeling. In [13], Haeberlen *et al.* suggest that environmental changes could be compensated by a simple linear transformation between RSSI values from different devices. However, Park *et al.* [25] claim that a linear transformation is insufficient for cross-device localization. Instead, they propose to use kernel estimation with wide kernel widths at the cost of single device localization performance degradation. In [18], fingerprints are recorded as more stable signal strength ratios between pairs of base stations and Dong *et al.* [10] proposed to use the difference between signal strengths across APs as a localization feature. However, as each AP adjusts its transmission power independently, the signal strength ratio (or the difference) remains unstable and unpredictable. WiGEM [12] is a learning-based approach using the Gaussian mixture model (GMM) and expectation maximization (EM) to estimate parameters of the WiFi propagation model on sniffers (or APs doubling as sniffers). It is robust to the device diversity and power level variability but requires knowledge of AP locations. Despite all of these techniques, GIFT leverages binary spatial RSSI gradients without any assumptions on signal prorogation models or signal strength transformations (e.g., linear) among devices, and is also complementary to the model-based fingerprint map construction approaches (e.g., WiGEM) for reducing the bootstrap effort.

Range-based approaches localize the user/device based on distance estimation, which can be achieved by measuring the received signal strength [5], [41], chirp-spread-spectrum [39], curve fitting [35], or time-of-arrival (ToA) [4], [23]. Signal propagation models are widely used in RSSI-based ranging approaches [5], [9], [22]. However, varied and complex interior structures in different indoor environments prevent the usage of a universal radio attenuation model; therefore, make such kind of systems less practical. In ToA-based ranging, time delays in signal propagation is leveraged to estimate distances between wireless nodes. With transmitters at known locations, difference in time of arrival of multiple RF signals is also used by TPS [4]. Although these techniques offer high localization accuracy, they require complicated processing in either software or hardware to ensure tight time synchronization and precise ranging, limiting their applicability.

Dead reckoning (DR) is also a well-studied localization topic for its infrastructure independency. These systems achieve positioning through data fusion from multiple inertial sensors, e.g., accelerometer, gyroscope, and magnetometer. However, the unstable human locomotion during walking and accumulated errors in inertial sensing makes DR hard to play well solely. Anomalies of indoor geomagnetic field, caused by local construction materials, also give rise to noisy direction sensing [7]. Complementary approaches that incorporate landmarks [37], map-constraints [26], and advanced human locomotion detection components [8], [20], [32], [40] were proposed recently to deal with problems in legacy DR systems. GIFT borrows these ideas and improves localization accuracy significantly.

III. Measurements and Observations

WiFi is the *de facto* standard for wireless Internet connectivity, with its signals ubiquitously exist in indoor environments. Due to wireless propagation model and the unique interior construction, indoor WiFi signals have been found to exhibit certain characteristics, e.g., location-specific RSSI. Such characteristics have been leveraged to build fingerprint maps to localize user/device [1], [26], [46]. Before proposing our main design, we first present some measurement and observation results on indoor WiFi signals.

A. Temporal Variation of WiFi Signals

Observations on the temporal variation of received signal strength were reported in WiFi's early days. With fixed transmit power, broadcasting signals from a WiFi router fluctuates in a time-variant indoor environment, e.g., the presence and absence of humans, the fluctuating indoor temperature and humidity. In most localization literature which leverages the RSSI fingerprint map, these factors are treated as random variables and could be eliminated through modeling or basic averaging.

Recently, with the advent of the high-density WiFi deployment and extensive research on wireless communication, new techniques are adopted in WiFi routers to meet the need of pervasive and high-performance wireless access. For example, in the new 802.11ac standard, beamforming is proposed to fortify RF connections of the AP/client link, and could also be used to optimize the RF spectrum and the overall network performance.

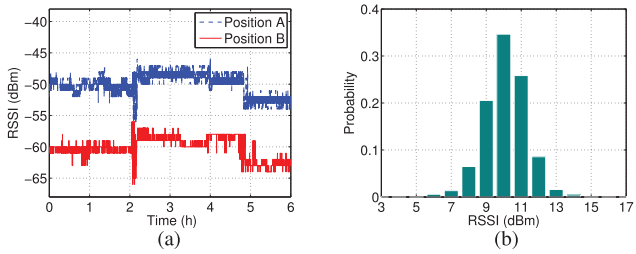

Fig. 1. Temporal variation of WiFi signals. (a) Absolute RSSI value. (b) RSSI gap.

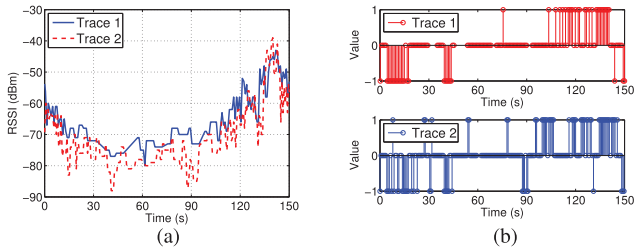

Fig. 2. Local disturbance of WiFi signals. (a) Absolute RSSI value. (b) Gradient-based map.

One typical optimization method used in off-the-shelf routers is to dynamically adjust the transmit power [14], [15] based on real-time wireless LAN conditions. Unlike the random impacts mentioned above, wireless signal strength variations caused by such modifications cannot be modeled easily due to the rapid and unpredictable changes of traffic load, the number of communication links and communication interference, etc.

We conducted experiments to verify the impact of the change of transmit power. Two smartphones 4 m apart continuously scan and record WiFi RSSI for hours in an office room. There are no object movements around during the experiment. RSSI observations from the same AP are recorded and plotted in Fig. 1(a), which shows the fluctuations of RSSI (with maximum change of 6 dBm) caused by adaptive transmit power adjustment. However, we find the RSSI gap between two smartphones remains positive and relatively stable. In Fig. 1(b), 81% RSSI differences between observations from two devices are in the range between 9 and 11 dBm.

B. Spatial–Temporal Variation of WiFi Signals

We further examine the spatial–temporal variation of WiFi signals. In this experiment, one user carries a smartphone and walks along a predefined path in an office environment at different times of the day. The smartphone keeps recording the WiFi RSSI during user walking. We plot the results to examine the difference among various traces.

Fig. 2(a) presents a high-dimensional perspective on the spatial–temporal variation of WiFi signals. A clear shift exists between two RSSI curves in Fig. 2(a). This is because the AP slightly increases its transmit power to cover a larger area in the morning when few connections have been established (Trace 1). In fact, the gap in between two curves reflects the temporal variation of RSSI at a fixed location (as presented in Section III-A).

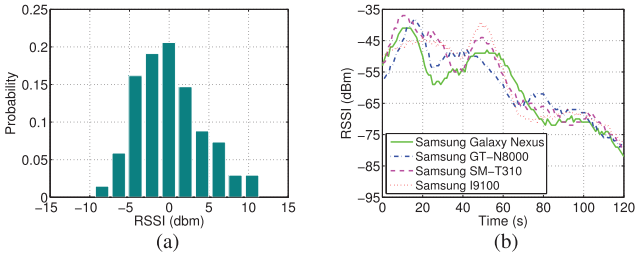

Fig. 3. (a) Human body effect. (b) Device diversity.

Although absolute RSSI values vary in two traces, two trends are similar. In Fig. 2(b), we use a sliding window to capture the trend of absolute RSSI values. Specifically, if the difference between RSSI values at two ends of the window is larger than a threshold δ (say 6 dBm), we generate an output of 1 (or -1 when the difference is smaller than $-\delta$). This way, the RSSI increase and decrease are represented by 1 and -1, respectively, in Fig. 2(b), and a 0 is generated when there is no obvious change. In Fig. 2(b), we find outputs of two traces are similar and more stable.

C. Human Body Effect and Device Diversity

Variations of RSSI are observed when the user is taking measurements while changing his/her orientation owing to the human body effect. In Fig. 3(a), we measure the signal strength toward four directions (e.g., East, West, North, and South) at a fixed location, and compute the RSSI deviations (i.e., the difference between the observed value and the mean). We repeat the experiment at 20 randomly selected locations in an office building. From Fig. 3(a), we find a symmetrical distribution of deviations centered at zero and in 79% of cases, RSSI deviations are less than 5 dBm though it could be as large as 11. In GIFT, we use Gaussian estimation to model this small-scale variation and perform gradient map construction through a statistical significance testing.

Fingerprint-based indoor localization systems also suffer from signal variation due to device heterogeneity. This is clearly demonstrated in Fig. 3(b), which shows the RSSI of one AP along exactly the same path using different smartphones. Compared with existing techniques for compensating for differences in RSSI values, GIFT leverages stable RSSI gradients without any signal strength transformations (e.g., linear) among devices.

As a brief summary, the time-varying signal strength makes it rather challenging to explore the WiFi signal directly, e.g., using absolute value-based fingerprinting techniques. The human body effect and device diversities further exaggerate the issue. Nevertheless, we find that the spatial gradient signal strength has favorable properties to serve as a localization modality.

IV. GIFT Overview

In this section, we present an overview of GIFT. GIFT consists of two main modules: the map construction and the GIFT engine. Fig. 4 shows the architecture of GIFT.

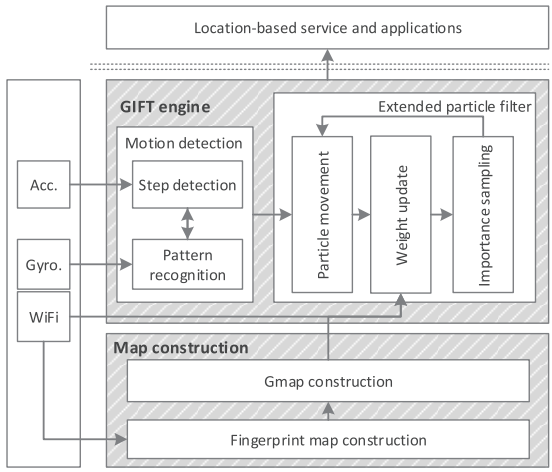

Fig. 4. GIFT architecture.

First, a Gmap is constructed. Different from existing absolute value-based fingerprint map, Gmap contains WiFi gradients of the indoor environment and can be stored either on the cloud or preinstalled on the clients (e.g., smartphones) before running GIFT. Gmap is derived from a traditional fingerprint map through significance testing. This way, GIFT is compatible with various fingerprint map building approaches including site survey [1], [46], crowdsourcing [26], and other advanced calibration methods with little human intervention [5], [44]. Gmap is used as input references by the GIFT engine which further compares user measurements and the pre-established WiFi gradient samples.

The GIFT engine continuously estimates locations of the user through a motion detection module and an EPF. The motion detection module recognizes user steps and learns the stride length based on the observations from the accelerometer and the gyroscope on smartphones. In addition, the accelerometer and the gyroscope are used to correct the noisy compass readings in indoor environment, thus providing reliable walking directions. Motion detection results are then forwarded to the EPF along with the pre-established Gmap. The location of the user, which is represented by a set of particles, is finally estimated and updated. We will detail each of the techniques in subsequent sections, followed by large-scale system evaluation.

V. Gradient-Based Map Construction

In this section, we present the calibration procedure of GIFT that includes a novel Gmap construction method.

A. Fingerprint Collection

We generate Gmap from an absolute value-based fingerprint map during the training phase of localization. Absolute value-based fingerprint map is universally used in indoor localization systems [1], [19], [26], [44], [46] with site survey [1], [46] being the main technique in fingerprint map construction. In spite of its reliability from standstill data collection, site surveying is strangled by the high cost on manpower and time. Efficient fingerprint map construction methods were proposed in literature

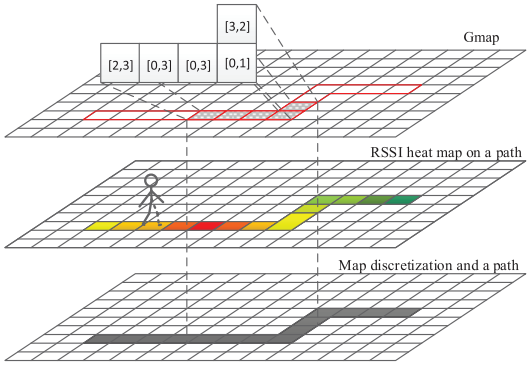

Fig. 5. Illustration of Gmap construction (with one AP).

during the past few years. For example, in [44], human motions are exploited to connect radio fingerprints. GIFT builds a Gmap by adding an additional layer above the absolute value-based fingerprint map, therefore, is compatible with legacy fingerprint map construction approaches. In addition, due to the stability of the Gmap, cost of the periodical fingerprint map calibration can be significantly reduced. Without loss of generality, we adopt the basic site surveying to illustrate the construction of Gmap.

Denoting the two-dimensional (2-D) indoor space by $\mathbb{G}$, we first discretize the area of interest $\mathbb{G}$ into grids and create paths which are composed of a series of consecutive grids based on the floor plan (the bottom layer in Fig. 5). For ease of presentation, we consider four basic walking directions (e.g., up, down, left, and right) with square grids. For a complex floor plan, hexagonal/octagonal grids can be leveraged to adaptive to nonvertical paths. In order to minimize the small-scale variations of RSSI caused by slightly movement of the user (order of wavelength, i.e., 12.5 and 6 cm in the 2.4 and 5 GHz WiFi frequencies, respectively), we set the grid length to 2 m, in accordance with the general performance of fingerprinting-based localization methods. Since the widths of most aisles in typical indoor environments are less than 3 m, one grid suffices. For rooms and wider hallways, multiple parallel and crossing paths are considered.

During site surveying, the surveyor scans the ambient WiFi signal n_g times at grid $g \in \mathbb{G}$ on a path and collects the signal strength from k_g APs. The corresponding measurement matrix $F_g \in \mathbb{R}^{k_g \times n_g}$ is then used to build the absolute value-based fingerprint map F (the middle layer in Fig. 5).

B. T-Test and Gmap Construction

The basic idea of generating Gmap is comparison of RSSI values at neighboring locations and replacing the original absolute RSSI values with the corresponding gradients. To determine the difference between fingerprint values at different locations, we borrow the idea from the significance testing in statistics and adopt *t*-test.

A *t*-test is a statistical hypothesis test which determines whether the null hypothesis (no difference between sample values) is to be rejected or accepted. Compared to other statistical hypothesis tests like *z*-test, *t*-test is more adaptable and is preferred for limited sample size with unknown standard deviation. Since the RSSI measurements from a specific AP follow a Gaussian distribution (as shown in Section III-C and reported in literature [25]), and n_g is not large enough in the training phase, *t*-test is a good means to compare two sets of fingerprint values so as to generate the Gmap.

Let F_g^j and $F_{g'}^j$ denote two sets of RSSI samples from AP j in the absolute value-based fingerprint map. Specifically, $\boldsymbol{F}_g^j = \{s_1^g, \ldots, s_{n_g}^g\}$ and $\boldsymbol{F}_{g'}^j = \{s_1^{g'}, \ldots, s_{n_{g'}}^{g'}\}$ are signal strength vectors collected at adjacent grids g and g', respectively. The mean of $\boldsymbol{F}_g^j$ and $\boldsymbol{F}_{g'}^j$ are denoted by $\mu_1 = \overline{F_g^j}$ and $\mu_2 = \overline{F_{g'}^j}$, respectively, and we test the following two-sided hypothesis:

$$\begin{aligned} H_0 &: \mu_1 = \mu_2 \\ H_1 &: \mu_1 \neq \mu_2. \end{aligned} \tag{1}$$

The *t*-statistic can be calculated as

$$t^j = \frac{\mu_1 - \mu_2}{\sqrt{\mathbf{S}_{\mu_1}\left(F_g^j, n_g\right) + \mathbf{S}_{\mu_2}\left(F_{g'}^j, n_{g'}\right)}} \tag{2}$$

where $\mathbf{S}_{\mu_1}(F_g^j, n_g) = S_{F_g^j}^2 / n_g$ and $\mathbf{S}_{\mu_2}(F_{g'}^j, n_{g'}) = S_{F_{g'}^j}^2 / n_{g'}$. $S_{F_g^j}^2 = \frac{1}{n_g - 1}\sum(F_g^j - \mu_1)^2$ and $S_{F_{g'}^j}^2 = \frac{1}{n_{g'} - 1}\sum(F_{g'}^j - \mu_2)^2$ are the unbiased estimators of the variance of the two sets of RSSI samples.

To test the significance, we set the significance level $\alpha = 0.1$ and the distribution of the test statistic can be approximated as an ordinary *t* distribution with the degrees-of-freedom (DoFs)

$$\text{d.f.} = \frac{\left(\mathbf{S}_{\mu_1}\left(F_g^j, n_g\right) + \mathbf{S}_{\mu_2}\left(F_{g'}^j, n_{g'}\right)\right)^2}{\frac{(\mathbf{S}_{\mu_1}(F_g^j, n_g))^2}{n_g - 1} + \frac{(\mathbf{S}_{\mu_2}(F_{g'}^j, n_{g'}))^2}{n_{g'} - 1}}. \tag{3}$$

Therefore, we can compute the cumulative distribution for *t* distribution with d.f. DoFs at the values in t^j. A cumulative density which is greater than $1 - \alpha$ indicates that the null hypotheses H_0 can be rejected with confidence (i.e., $\mu_1 \neq \mu_2$), and accepted (i.e., $\mu_1 = \mu_2$) otherwise. Note that although the calculated cumulative density varies with different α, subtle variations on the test results are observed when $0.05 \leq \alpha \leq 0.15$. In GIFT, these variations can be efficiently alleviated through the EPF due to its probabilistic nature.

On the basis of significance test, we compute the binary gradient of AP j between location g and g' as

$$b^j(g, g') = \begin{cases} 1, & H_0 \text{ is accepted} \\ 2, & H_0 \text{ is rejected and } \mu_1 \geq \mu_2 \\ 0, & H_0 \text{ is rejected and } \mu_1 < \mu_2. \end{cases} \tag{4}$$

$b^j(g, g')$ in (4) characterizes the RSSI changes between neighboring grids and it is easy to prove $b(g, g') + b(g', g) = 2$ [e.g., if $b(g, g') = 0$, then $b(g', g) = 2$]. The gradient-based fingerprint value Gmap_g at position g can be represented as a $k_g \times 2$ matrix which stores the binary gradient values $b^j(g, g')$ of k_g different APs. Since $b(g, g') + b(g', g) = 2$, we only consider grid g' which is located either right above or to the left of grid g

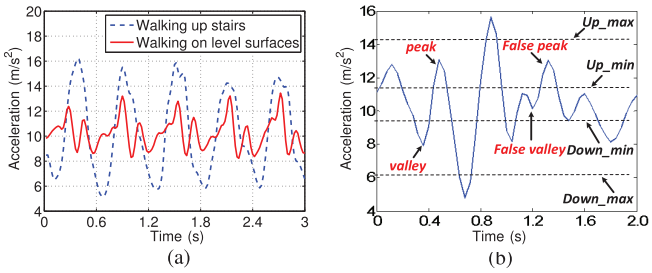

Fig. 6. Accelerometer readings during walking. (a) Level walking versus walking upstairs. (b) Peak detection.

and included the corresponding two gradient values in Gmap_g (i.e., the two columns) to reduce the size of the map.

Finally, Gmap is obtained as a union of Gmap_g as

$$\mathrm{Gmap} = \bigcup_g \mathrm{Gmap}_g, g \in \mathbb{G}. \tag{5}$$

A Gmap captures gradient values of RSSI from one specific AP that is shown in Fig. 5. Particularly, if the grid right above or on top of g is not on walking paths, we set the corresponding gradient value to 3.

VI. GIFT Engine

The GIFT engine consists of a motion detection module and an EPF.

A. Motion Detection

This module recognizes user mobility pattern and steps using sensor data from the IMU, i.e., accelerometers, gyroscopes, and compass. In GIFT, we assume the user is holding the smartphone steady in his hand when requesting his location, which is a likely indoor localization scenario.

User mobility pattern recognition, serving as an input of the motion model in the EPF, detects whether the user is *standing still*, *walking on level surfaces*, or *walking up/down stairs*. For motion detection, we first divide accelerometer data into several segments, then extract features from three-axes accelerometer readings contained within each segment and adopt a decision tree-based classification algorithm. Specifically, the algorithm first decides whether the user is moving. If so, it then determines if the user is walking on level surfaces or walking up/down stairs. After that, different parameters (e.g., thresholds) are used to help extract steps.

The duration of each segment is set to 3 s, enough to capture multiple steps involved in activities. Features we use include the average acceleration, standard deviation of acceleration, and the average absolute difference between each reading and the average value. An example of accelerometer's Z-axis readings is shown in Fig. 6(a) where we can easily differentiate the output of *walking on level surfaces* from *walking upstairs*. Specifically, the standard deviation and the average absolute difference of walking upstairs are almost $3\times$ higher than the output during level walking $(3.39, 3.06$ vs. $1.21, 0.96)$.

If the user is standing still, GIFT holds the current location estimation, otherwise it will be continuously running the step detection algorithm based on the accelerometer readings. Previously developed algorithms can reliably detect user steps [26], [27]. GIFT borrows these algorithms with a few minor adjustments. First, in the step detection algorithm, a low-pass finite impulse response (FIR) digital filter is used to remove the high frequency noise and spikes in raw acceleration readings. Since the step frequency in indoor environments mostly ranges from 1 Hz (slow walk) to 3 Hz (walking briskly or running) [24], we set the cut-off frequency of the filter to 3 Hz. After preprocessing, a peak detection algorithm is applied on the filtered signal to identify steps.

Four thresholds are used in the algorithm to detect the peak and valley. $\mathrm{Up}_{\min}$ and $\mathrm{Down}_{\min}$ are used to remove the interference of small peaks and valleys caused by a slight sways of the phone. Similarly, $\mathrm{Up}_{\max}$ and $\mathrm{Down}_{\max}$ are used to remove the interference of heavy bouncing of the phone. Here, we use the same value used in [33] to set the threshold. Once the duration of one candidate step is smaller than 0.3 s or larger than 1 s, we consider it as a false step. Fig. 6(b) shows an example of filtered accelerometer readings with automatically detected peaks. Putting all these components together, our step detection algorithm achieves a 3% false positive rate and 2% false negative rate.

B. Extended Particle Filter

All of the motion detection results are combined into an EPF to estimate the user's location. Particle filtering, also known as Monte Carlo methods, is commonly used in tracking-based localization systems [26], [30]. In this paper, particles are uniformly driven by the fused direction sensing results and weights of particles are updated during the movement based on the comparison results between WiFi RSSI observations and Gmap. User location is simultaneously estimated via a probability distribution of particles with different weights. In what follows, we describe the details of particle initialization, movement, weight update, and importance sampling.

1) Particle Initialization and the Motion Model: In EPF, the state of a particle $\mathbf{p_i}$ is a 4-tuple consisting of its current location l_i, weight w_i, and two stride length coefficients a_i and b_i. At the very beginning of the localization process with no *a prior* knowledge of the user's initial position, N particles are generated and uniformly distributed on all paths with an equal weight $w_i = \frac{1}{N}, i \in [1, N]$.

After initialization, all particles move once a step is detected by the motion detection module. In each movement, EPF first estimates the stride length of the user and then updates the location of each particle toward the moving direction. Although stride length varies with users and is affected by walking speed, a linear function of step frequency is adaptive to capture the variation [20]. In EPF, we define the stride length $sl_i = a_i f + b_i$ where f is the step frequency obtained by the motion detection module and a_i, b_i are two coefficients that needed to be estimated. Each particle i in EPF is associated with a fixed pair of a, b (i.e., a_i, b_i). During initialization, values of a_i and b_i are set based on a generic stride length model where a_i and b_i are

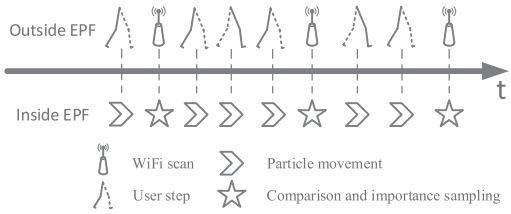

Fig. 7. Illustration of particle movement and comparison.

sampled from a Gaussian distribution with means of 2 and 4 and variance of 0.8 and 0.4, respectively. A nonzero variance is introduced here to capture the possible error of stride length estimation. Note that similar values of a_i and b_i can still be applied due to the randomness of particle moving distance. Via importance sampling (discussed in Section VI-B2), EPF eliminates those particles with improper stride length coefficients, and thus estimates location and stride length simultaneously as the user continues walking.

The moving direction of particles is primarily generated based on the absolute heading direction readings reported by the smartphone. It is often a fusion result from compass and gyroscope. In consideration of the magnetic interferers in indoor environments, we adopt the iterative magnetic triangulation method [27] (assuming a single ambient interferer) to further correct the raw direction sensing results.[1]

2) Weight Update and Importance Sampling: As mentioned above, particles $i, i \in [1, N]$ move for sl_i toward the user's moving direction once a step is detected. At the same time, GIFT periodically scans ambient WiFi signals with a fixed frequency f_s. A sequence diagram of EPF is shown in Fig. 7.

Two series of actions can be found in Fig. 7: user steps and WiFi scans. Unlike WiFi scanning, the frequency of steps changes with time. Similarly, in EPF, particle movement is triggered by steps while the gradient calculation, weight update, and importance sampling are conducted on a per-scan basis.[2]

a) Gradient calculation: The EPF first performs RSSI comparison between two consecutive WiFi scans, based on which weights of particles are updated. Let R_g and $R_{g'}$ denote RSSI samples of two consecutive scans, then RSSI difference (dissimilarity) $d^j_{gg'}$ between two scan results is computed as $d^j_{gg'} = \|R^j_g - R^j_{g'}\|_1$ where $\|\cdot\|_1$ is the Euclidean distance between two RSSI values and j is the AP included in both R_g and $R_{g'}$. The EPF then computes b^j_0, the binary gradient of AP j between R_g and $R_{g'}$ based on the calculated dissimilarity $d^j_{gg'}$. Specifically, if $d^j_{gg'}$ is greater than a predefined threshold δ, then the binary gradient $b^j_0 = 2$, if $d_j \leq -\delta$, $b^j_0 = 0$, else $b^j_0 = 1$. δ is determined based on fingerprint samples collected at a given location. In order to avoid the small-scale RSSI variations, we set δ to 6 in GIFT based on the observation of Fig. 3(a). Similar solutions have been adopted elsewhere [37], [44] as well.

b) Weight update and importance sampling: After obtaining the binary gradient values of all APs after each scan,

[1]Key intuition of IMT is to decompose the measured magnetic vector into the earth's magnetic vector ($\boldsymbol{G}$) and the interference vector ($\boldsymbol{I}$), and adjust the direction of $\boldsymbol{G}$ until all the $\boldsymbol{I}$ vectors intersect at the same point.

[2]Particularly, if the user is standing still, EPF holds without weight update and importance sampling.

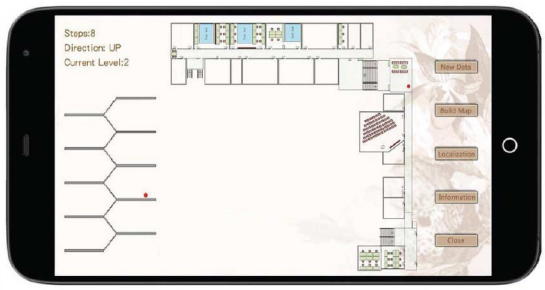

Fig. 8. Screenshot of GIFT application.

EPF updates weights of particles based on their similarities between calculated gradient values and the preinstalled Gmap. Specifically, for particle $\mathbf{p_i}$ located at position l_i, EPF first extracts Gmap_{l_i} and compares it with the gradient value b_0. Note that particles may be located at nonadjacent grids during two consecutive WiFi scans, and hence we replace Gmap_{l_i} with the average value $\overline{\mathrm{Gmap}_{\mathbf{g}}}$ across the entire traveling grids $\mathbf{g}$ of particles between two WiFi scans. Then, Euclidean distance is calculated between Gmap_{l_i} and b_0, and the weight of particle is set to $w_i = e^{-\frac{(\sum_j \|\mathrm{Gmap}^j_{l_i} - b^j_0\|_1)^2}{2\sigma^2}}$ where j refers to the shared AP between Gmap_{l_i} and b_0, and σ is a parameter that reflects the overall disturbance intensity of WiFi gradient. In addition, when the particles are moving toward the walls according to the direction sensing result, their weights will be significantly reduced (but not eliminated). Finally, weight-based importance sampling of particles is conducted. Since the distribution of particles reflects the likelihood of the real location of the user, the estimated location is set to the weighted averaged point of all particles' positions using their own weights.

VII. Evaluation

We have implemented GIFT on Android platforms and evaluated it in a five-story office building with a testing area of about $8000\,\mathrm{m}^2$. Detailed evaluation settings and implementation are described in Section VII-A. Section VII-B presents experimental results of GIFT in environments with both relatively stable and dynamic WiFi signals. Localization performance of GIFT on multiple devices is presented in Section VII-C.

A. Implementation

1) Settings: We implemented GIFT on the Android platform including a tablet and several smartphones. A screenshot of the GIFT application is shown in Fig. 8. Users can adjust the zoom level to change the size of the indoor floor plan in the middle of the screen. GIFT offers several modes: the map construction mode to guide the user to collect values on each path on the map and the localization mode to test the system accuracy.

2) Map Construction Mode: Before running GIFT, we first built the RSSI fingerprint map F as well as Gmap. Specifically, once the construction mode is chosen, paths are shown on the screen and the user can choose each path by

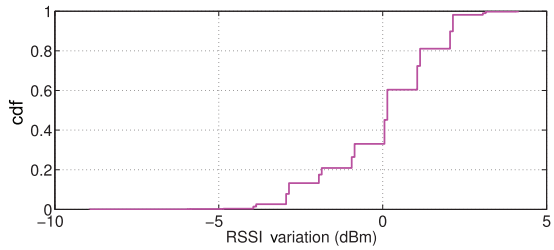

Fig. 9. RSSI variation in a dynamic environment.

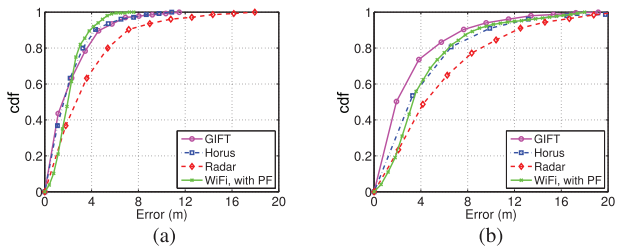

Fig. 10. Localization performance. (a) Static WiFi environment. (b) Dynamic WiFi environment.

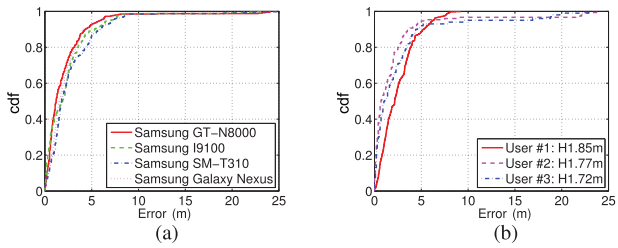

Fig. 11. Results from different devices and users. (a) Different devices. (b) Different users.

clicking on it. During user walking, GIFT automatically collects RSSI data on each path. It records timestamps at both the beginning and end of a walk and maps the fingerprints onto the floor plan through a simple linear interpolation. Gmap is then generated following the procedures presented in Section V.

3) Localization Mode: In the localization mode, the mobile client performs continuous IMU sampling at 50 Hz, WiFi scan at 1 Hz, and updates the estimated location of the user through the online EPF. In our experiment, we set the number of particles to 2000. In order to obtain ground truth positions of the user, we set landmarks every other meter along the path, and users tap on the screen to record timestamps when they pass by each landmark.

4) Microbenchmark: We use two classical fingerprint-based localization approaches, Radar [1] and Horus [46], and a particle filtering-based tracking method [30] as benchmarks in experiments. Radar [1] is an early fingerprinting system which uses a deterministic RSSI fingerprint for each location, whereas Horus [46] adopts a probabilistic RSSI map and a maximum-likelihood-based approach. Although new fingerprinting techniques have been proposed in recent years, they either focus on the prelocalization training process [44] or achieve similar (or slightly worse [5]) positioning accuracy to these two legacy methods. To further evaluate the performance of using gradient map, we also implemented a particle filtering-based tracking method [30], which takes the fingerprint map of absolute value of RSSI and floor plan as inputs. Step detection algorithm in GIFT is also leveraged for particle movement and weight updating. We collected more than 300 walking traces and ignore localization results in the first 3 s of each trace due to the time particles spend to converge. Location requests were randomly made in Radar and Horus during each walking trace.

B. Performance in Static and Dynamic Environments

We first conducted experiments in a static environment with customized deployment of early WiFi APs with fixed transmit power. Cumulative distribution function (cdf) of localization error of all traces is shown in Fig. 10(a). We can see that GIFT, Horus, and WiFi RSSI-based particle filtering method achieve comparable performance in terms of localization error, outperforming the localization accuracy of Radar. For example, the 80 percentile accuracy of GIFT, WiFi particle filtering, Horus, and Radar are 3.6, 2.9, 3.3, and 5.4 m, respectively.

To further examine the accuracy and robustness of the four algorithms, we tested them in a dynamic environment with predeployed, ARM-enabled WiFi APs. To verify the RSSI variations in the dynamic environment, we collected RSSI of multiple APs at a fixed location for 4 h, and aligned all measurements by removing the mean RSSI value of each AP during the monitoring period. The cdf of RSSI variations of all APs is shown in Fig. 9 in which an RSSI difference of as high as 9 dB can be observed. In this experiment, we built Gmap in the morning and ran localization systems in the afternoon after 1 week.

Compared to Fig. 10(a), we find localization performance of all four system degrades in Fig. 10(b). This is owing to the fact of fluctuant transmit power of WiFi APs. However, GIFT is more reliable in the dynamic environment due to the gradient-based fingerprinting. For example, in Fig. 10(b), the 80 percentile accuracy of Horus is 6.58 m, which has a 99.4% performance degradation over that in the static environment. However, for GIFT, the performance degradation of the 80 percentile accuracy is only 55.6% (5.6 m vs. 3.6 m) .

C. Robustness Among Different Devices and Users

To examine GIFT's robustness, we conducted experiments using heterogeneous devices and tested GIFT among multiple users with different heights that may have various stride lengths and walking speeds. All experiments were conducted in the static environment. The cdf of the localization error for four devices and three users are plotted in Fig. 11(a) and (b), respectively. From both figures, we can see that the cdf curves are very close, and they are consistent with the experimental results in Section VII-B. This demonstrates the robustness and practicality of GIFT. On the contrary, fingerprint-based localization approaches (e.g., Radar and Horus) yield a much worse accuracy while localizing a new mobile device that has never been used to generate the model. We refer [36], [21], and [5] for detailed evaluation results.

We also found several practical issues and limitations of GIFT during evaluation. For example, as GIFT uses compute-intensive particle filter as the localization engine, the energy

consumption of the system is relatively high. In our experiments, the runtime current of Samsung GT-N8000 reaches as high as 840 mA when the particle filter is running. Therefore, it is worth investigating how to reduce the energy consumption while enjoying the benefits of using gradient maps. For example, it is interesting to investigate how to reduce the energy cost by scheduling the calculation [47].

VIII. Conclusion

In this paper, we have proposed GIFT, an indoor localization system leveraging Gmap. We first presented key observations of indoor WiFi signals and then presented the design of GIFT based on the robust gradient-based RSSI map. Gradient-based map is a sublayer compatible with various wireless networks. Compared to legacy fingerprinting methods, GIFT is more adaptive to the time-variant indoor wireless signals and device heterogeneity, and therefore could effectively reduce the cost of maintenance of the fingerprint map. We implemented GIFT on off-the-shelf devices and extensively evaluated its performance in indoor environments with dynamic WiFi signals. Our experimental results confirm the high accuracy and robustness of GIFT.

References

[1] P. Bahl and V. N. Padmanabhan, "RADAR: An in-building RF-based user location and tracking system," in *Proc. IEEE INFOCOM*, 2000, pp. 775–784.

[2] J. Chen, J. Li, and T. Lai, "Trapping mobile targets in wireless sensor networks: An energy-efficient perspective," *IEEE Trans. Veh. Technol.*, vol. 62, no. 7, pp. 3287–3300, Sep. 2013.

[3] Y. Chen, D. Lymberopoulos, J. Liu, and B. Priyantha, "FM-based indoor localization," in *Proc. ACM MobiSys*, 2012, pp. 169–182.

[4] X. Cheng, A. Thaeler, G. Xue, and D. Chen, "TPS: A time-based positioning scheme for outdoor wireless sensor networks," in *Proc. IEEE INFOCOM*, 2004, pp. 2685–2696.

[5] K. Chintalapudi, A. P. Iyer, and V. N. Padmanabhan, "Indoor localization without the pain," in *Proc. ACM MobiCom*, 2010, pp. 173–184.

[6] K. H. Choi, W.-S. Ra, S.-Y. Park, and J. B. Park, "Robust least squares approach to passive target localization using ultrasonic receiver array," *IEEE Trans. Ind. Electron.*, vol. 61, no. 4, pp. 1993–2002, Apr. 2014.

[7] J. Chung, M. Donahoe, C. Schmandt, I.-J. Kim, P. Razavai, and M. Wiseman, "Indoor location sensing using geo-magnetism," in *Proc. ACM MobiSys*, 2011, pp. 141–154.

[8] I. Constandache, R. R. Choudhury, and I. Rhee, "Towards mobile phone localization without war-driving," in *Proc. IEEE INFOCOM*, 2010, pp. 1–9.

[9] I. Constandache, S. Gaonkar, M. Sayler, R. Choudhury, and L. Cox, "EnLoc: Energy-efficient localization for mobile phones," in *Proc. IEEE INFOCOM*, 2009, pp. 2716–2720.

[10] F. Dong, Y. Chen, J. Liu, Q. Ning, and S. Piao, "A calibration-free localization solution for handling signal strength variance," in *Proc. Int. Conf. Mobile Entity Local. Tracking GPS-Less Environ.*, 2009, pp. 79–90.

[11] A. Eleryan, M. Elsabagh, and M. Youssef, "Synthetic generation of radio maps for device-free passive localization," in *Proc. IEEE Globecom*, 2011, pp. 1–5.

[12] A. Goswami, L. E. Ortiz, and S. R. Das, "WiGEM: A learning-based approach for indoor localization," in *Proc. ACM CoNEXT*, 2011, pp. 3.

[13] A. Haeberlen, E. Flannery, A. Ladd, A. Rudys, D. Wallach, and L. Kavraki, "Practical robust localization over large-scale 802.11 wireless networks," in *Proc. ACM MobiCom*, 2004, pp. 70–84.

[14] Aruba Networks Inc. (2015). *Aruba 220 Series Access Points* [Online]. Available: www.arubanetworks.com/products/networking/access-points/220-series/

[15] Cisco Inc. (2015). *Cisco Aironet 1240AG Series Access Points* [Online]. Available: http://www.cisco.com/c/en/us/products/collateral/collaboration-endpoints/unified-ip-phone-7900-series/product_data_sheet0900aecd8031c844.html

[16] Netgear Inc.. (2015). *Adaptive Radio Management* [Online]. Available: http://www.downloads.netgear.com/files/GDC/WFS709TP/Adaptive%20Radio%20Management.pdf

[17] S. J. Kim and B. K. Kim, "Dynamic ultrasonic hybrid localization system for indoor mobile robots," *IEEE Trans. Ind. Electron.*, vol. 60, no. 10, pp. 4562–4573, Oct. 2013.

[18] M. B. Kjærgaard, "Indoor location fingerprinting with heterogeneous clients," *Pervasive Mobile Comput.*, vol. 7, no. 1, pp. 31–43, Feb. 2011.

[19] B. Li, T. Gallagher, A. G. Dempster, and C. Rizos, "How feasible is the use of magnetic field alone for indoor positioning?" in *Proc. Int. Conf. Indoor Position. Indoor Navig. (IPIN)*, 2012, pp. 1–9.

[20] F. Li, C. Zhao, G. Ding, J. Gong, C. Liu, and F. Zhao, "A reliable and accurate indoor localization method using phone inertial sensors," in *Proc. ACM UbiComp*, 2012, pp. 421–430.

[21] L. Li, G. Shen, C. Zhao, T. Moscibroda, J. Lin, and F. Zhao, "Experiencing and handling the diversity in data density and environmental locality in an indoor positioning service," in *Proc. ACM MobiCom*, 2014, pp. 459–470.

[22] K. Lin, A. Kansal, D. Lymberopoulos, and F. Zhao, "Energy-accuracy trade-off for continuous mobile device location," in *Proc. ACM MobiSys*, 2010, pp. 285–298.

[23] K. Liu, X. Liu, and X. Li, "Guoguo: Enabling fine-grained indoor localization via smartphone," in *Proc. ACM MobiSys*, 2013, pp. 235–248.

[24] A. Pachi and T. Ji, "Frequency and velocity of people walking," *Struct. Eng.*, vol. 83, no. 3, pp. 36–40, 2005.

[25] J.-G. Park, D. Curtis, S. Teller, and J. Ledlie, "Implications of device diversity for organic localization," in *Proc. IEEE INFOCOM*, 2011, pp. 3182–3190.

[26] A. Rai, K. K. Chintalapudi, V. N. Padmanabhan, and R. Sen, "Zee: Zero-effort crowdsourcing for indoor localization," in *Proc. ACM MobiCom*, 2012, pp. 293–304.

[27] N. Roy, H. Wang, and R. Roy Choudhury, "I am a smartphone and I can tell my user's walking direction," in *Proc. ACM Mobisys*, 2014, pp. 329–342.

[28] S. Saad and Z. Nakad, "A standalone RFID indoor positioning system using passive tags," *IEEE Trans. Ind. Electron.*, vol. 58, no. 5, pp. 1961–1970, May 2011.

[29] G. Shen, Z. Chen, P. Zhang, T. Moscibroda, and Y. Zhang, "Walkie-Markie: Indoor pathway mapping made easy," in *Proc. USENIX Netw. Syst. Des. Implement. (NSDI)*, 2013, pp. 85–98.

[30] Y. Shu, C. Bo, G. Shen, C. Zhao, L. Li, and F. Zhao, "Magicol: Indoor localization using pervasive magnetic field and opportunistic WiFi sensing," *IEEE J. Sel. Areas Commun.*, vol. 33, no. 7, pp. 1443–1457, Jul. 2015.

[31] Y. Shu, P. Coue, Y. Huang, J. Zhang, P. Cheng, and J. Chen, "Demo: G-Loc: Indoor localization leveraging gradient-based fingerprint map," in *Proc. IEEE INFOCOM*, Apr. 2014, pp. 129–130.

[32] Y. Shu, K. G. Shin, T. He, and J. Chen, "Last mile navigation using smartphones," in *Proc. ACM MobiCom*, 2015, pp. 512–524.

[33] M. Susi, V. Renaudin, and G. Lachapelle, "Motion mode recognition and step detection algorithms for mobile phone users," *Sensors*, vol. 13, no. 2, pp. 1539–1562, 2013.

[34] A. Varshavsky, E. de Lara, J. Hightower, A. LaMarca, and V. Otsason, "GSM indoor localization," *Pervasive Mobile Comput.*, vol. 3, no. 6, pp. 698–720, 2007.

[35] B. Wang, S. Zhou, W. Liu, and Y. Mo, "Indoor localization based on curve fitting and location search using received signal strength," *IEEE Trans. Ind. Electron.*, vol. 62, no. 1, pp. 572–582, Jan. 2015.

[36] C.-H. Wang et al., "Robust Wi-Fi location fingerprinting against device diversity based on spatial mean normalization," in *Proc. Asia Pac. Signal Inf. Process. Assoc. Annu. Summit Conf. (APSIPA)*, 2013, pp. 1–4.

[37] H. Wang, S. Sen, A. Elgohary, M. Farid, M. Youssef, and R. R. Choudhury, "No need to war-drive: Unsupervised indoor localization," in *Proc. ACM MobiSys*, 2012, pp. 197–210.

[38] J. Wang, Q. Gao, Y. Yu, P. Cheng, L. Wu, and H. Wang, "Robust device-free wireless localization based on differential RSS measurements," *IEEE Trans. Ind. Electron.*, vol. 60, no. 12, pp. 5943–5952, Dec. 2013.

[39] J. Wang, Q. Gao, Y. Yu, H. Wang, and M. Jin, "Toward robust indoor localization based on bayesian filter using chirp-spread-spectrum ranging," *IEEE Trans. Ind. Electron.*, vol. 59, no. 3, pp. 1622–1629, Mar. 2012.

[40] O. Woodman and R. Harle, "Pedestrian localization for indoor environments," in *Proc. ACM UbiComp*, 2008, pp. 114–123.

[41] K. Wu, J. Xiao, Y. Yi, M. Gao, and L. M. Ni, "FILA: Fine-grained indoor localization," in *Proc. IEEE INFOCOM*, 2012, pp. 2210–2218.

[42] P. Yang and W. Wu, "Efficient particle filter localization algorithm in dense passive RFID tag environment," *IEEE Trans. Ind. Electron.*, vol. 61, no. 10, pp. 5641–5651, Oct. 2014.
[43] P. Yang, W. Wu, M. Moniri, and C. Chibelushi, "Efficient object localization using sparsely distributed passive RFID tags," *IEEE Trans. Ind. Electron.*, vol. 60, no. 12, pp. 5914–5924, Dec. 2013.
[44] Z. Yang, C. Wu, and Y. Liu, "Locating in fingerprint space: Wireless indoor localization with little human intervention," in *Proc. ACM MobiCom*, 2012, pp. 269–280.
[45] S. Yoon, K. Lee, and I. Rhee, "FM-based indoor localization via automatic fingerprint DB construction and matching," in *Proc. ACM MobiSys*, 2013, pp. 207–220.
[46] M. Youssef and A. K. Agrawala, "The horus WLAN location determination system," in *Proc. ACM MobiSys*, 2005, pp. 205–218.
[47] H. Zhang, P. Cheng, L. Shi, and J. Chen, "Optimal DoS attack scheduling in wireless networked control System," *IEEE Trans. Control Syst. Technol.*, DOI: 10.1109/TCST.2015.2462741.
[48] Y. Zhang, S. He, and J. Chen, "Data gathering optimization by dynamic sensing and routing in rechargeable sensor networks," *IEEE/ACM Trans. Netw.*, DOI: 10.1109/TNET.2015.2425146.

Yuanchao Shu (S'12–M'15) received the Ph.D. degree in control science and engineering from Zhejiang University, Hangzhou, China, in 2015.

He is currently an Associate Researcher with Microsoft Research Asia, Beijing, China. From 2013 to 2015, he was a Joint Ph.D. student with the University of Michigan, Ann Arbor, MI, USA. His research interests include cyber-physical systems, mobile computing, wireless sensor network, and big data analysis.

Dr. Shu is a member of the Association for Computing Machinery (ACM). He has authored or coauthored more than ten papers published in premier journals and conference proceedings, including the IEEE JOURNAL ON SELECTED AREAS IN COMMUNICATION, IEEE TRANSACTIONS ON MOBILE COMPUTING, IEEE TRANSACTIONS ON PARALLEL AND DISTRIBUTED SYSTEMS, ACM MobiCom, and the IEEE INFOCOM. He was the recipient of the IBM Ph.D. Fellowship and the INFOCOM'14 Best Demo Award.

Yinghua Huang received the B.E. degree in automation from Shanghai Jiaotong University, Shanghai, China, in 2012, and the M.S. degree in control science and engineering from Zhejiang University, Hangzhou, China, in 2015.

He is currently a Working Staff Member with Huawei, Shenzhen, China. His research interests include mobile social networks, delay-tolerant networks, and mobile computing.

Jiaqi Zhang received the Bachelor's degree in control science and engineering from Zhejiang University, Hangzhou, China, in 2013, where he is currently working toward the Master's degree in control science and engineering.

His research interests include mobile computing and sensor networks.

Philippe Coué received the Master's degree in telecommunications from the Insa Lyon Engineering School, Lyon, France, in 2013.

He is currently a Data Intelligence Consultant working all over Europe (Paris, Budapest, and Copenhagen) on global transformation of international telecom operator information systems. He was a Joint Student with the Department of Control, Zhejiang University, Hangzhou, China, in 2013. His research interests include mobile computing, wireless sensor networks, and big data analysis.

Mr. Coué was the recipient of the INFOCOM'14 Best Demo Award.

Peng Cheng (M'10) received the B.E. degree in automation and the Ph.D. degree in control science and engineering, in 2004 and 2009, respectively, from Zhejiang University, Hangzhou, China.

He is currently an Associate Professor with the Department of Control Science and Engineering, Zhejiang University. His research interests include networked sensing and control, cyber-physical systems, and robust control.

Dr. Cheng is the Guest Editor for the IEEE TRANSACTIONS ON CONTROL OF NETWORK SYSTEMS. He serves as an Associate Editor for *Wireless Networks* and the *International Journal of Communication Systems*. He served as Publicity Co-Chair for the IEEE MASS 2013 and Local Arrangement Chair for ACM MobiHoc 2015.

Jiming Chen (M'08–SM'11) received the B.Sc. and Ph.D. degrees in control science and engineering from Zhejiang University, Hangzhou, China, in 2000 and 2005, respectively.

He was a Visiting Researcher at INRIA, France, in 2006, the National University of Singapore, Singapore, in 2007, and the University of Waterloo, Waterloo, ON, Canada, from 2008 to 2010. Currently, he is a Full Professor with the Department of Control Science and Engineering and Vice Director of the State Key Laboratory of Industrial Control Technology and Institute of Industrial Process Control, Zhejiang University. His research interests include sensor networks and networked control.

Dr. Chen currently serves as an Associate Editor for several international journals, including the IEEE TRANSACTIONS ON PARALLEL AND DISTRIBUTED SYSTEMS, the IEEE NETWORK, and the IEEE TRANSACTIONS ON CONTROL OF NETWORK SYSTEMS. He was a Guest Editor of the IEEE TRANSACTIONS ON AUTOMATIC CONTROL.

Kang G. Shin (LF'12) received the B.S. degree in electronics engineering from Seoul National University, Seoul, Korea, in 1970, and the M.S. and Ph.D. degrees in electrical engineering from Cornell University, Ithaca, NY, USA, in 1976 and 1978, respectively.

He is the Kevin and Nancy O'Connor Professor of Computer Science with the Department of Electrical Engineering and Computer Science, University of Michigan, Ann Arbor, MI, USA. He has supervised the completion of 75 Ph.D.s, and authored/coauthored more than 830 technical articles, a textbook, and more than 30 patents or invention disclosures. His research interests include QoS-sensitive computing and networking as well as on embedded real-time and cyber-physical systems. He was a Co-Founder of a couple of startups and also licensed some of his technologies to industry.

Prof. Shin was the recipient of the Best Paper Awards from the 2011 ACM MobiCom, the 2011 IEEE ICAC, the 2010 and 2000 USENIX ATC, as well as the 2003 IEEE Communications Society William R. Bennett Prize Paper Award, and the 1987 Outstanding IEEE Transactions of Automatic Control Paper Award. He was also the recipient of the Research Excellence Award in 1989, the Outstanding Achievement Award in 1999, the Distinguished Faculty Achievement Award in 2001, and the Stephen Attwood Award in 2004 from the University of Michigan (the highest honor bestowed to Michigan Engineering faculty), a Distinguished Alumni Award of the College of Engineering, Seoul National University, Seoul, Korea, in 2002; the 2003 IEEE RTC Technical Achievement Award; and the 2006 Ho-Am Prize in Engineering (the highest honor bestowed to Korean-origin engineers).